THE AMERICAN MINERALOGIST, VOL. 53, SEPTEMBER-OCTOBER, 1968

INESITE FROM THE BROKEN HILL LODE, NEW SOUTH WALES, AUSTRALIA

WILLIAM R. RYALL[1] AND IAN M. THREADGOLD, *Department of Geology and Geophysics, The University of Sydney, Sydney, Australia.*

ABSTRACT

Inesite occurs as acicular, radiating aggregates in post-ore, fracture-filled veins within the Broken Hill lode, its associated minerals are calcite, apophyllite and chlorite.

Broken Hill inesites have higher iron and correspondingly lower manganese contents than those reported from other localities. Chemical analyses of samples from three localities range between: SiO_2 45.48–45.58, MnO 33.24–34.38, FeO 2.46–3.33, CaO 8.48–8.73, MgO 0.10–0.23, Al_2O_3 0.19–0.25, Na_2O 0.07–0.30, K_2O 0.07–0.18, H_2O^+ 6.43–6.63, H_2O^- 2.10–2.22 wt.%.

Unit-cell dimensions of three samples determined from X-ray precession photographs range between: $a=8.927$–8.929 Å, $b=9.239$–9.245, $c=11.946$–11.954, $\alpha=91°48'$–$91°58'$, $\beta=132°35'$–$132°38'$, $\gamma=94°09'$–$94°22'$.

Space group is $P\bar{1}$ and there is one formula unit of $[Mn_7Ca_2(OH)_2(H_2O)_6]$ $Si_{10}O_{28}$ per unit cell. The principal X-ray lines are: 9.16 (10) (010), 2.92 (8) ($1\bar{3}0$), 2.84 (8) ($2\bar{2}0$), 2.73 (7) ($13\bar{2}$), 2.19 (6) ($3\bar{3}3$), 4.59 (5) (020), 4.01 (5) ($1\bar{2}0$).

Refractive indices, determined by the double variation method, range between: $\alpha=1.6178$–1.6183, $\beta=1.6384$–1.6390, $\gamma=1.6519$–1.6526. Biaxial negative, $2V$ range: ortho. 74°54′–76°54′; cono. 75°30′–76°40′. Orientation $\alpha\wedge c=74°$, $\beta\wedge c=32°$, $\gamma\wedge c=62°$. Dispersion: $r>v$, weak; pleochroism: nil.

A study of the thermal decomposition of inesite in air shows that despite the loss of practically all the water and hydroxyl below 500°C the inesite chain-structure still exists to 705°–710°C, at which temperature it transforms to a "rhodonite-like" structure that, at about 800°C is itself transformed to a "bustamite-like" structure. Near 800°C braunite appears and coexists with the "bustamite-like" phase but decreases in importance beyond 1050°C, at which temperature cristobalite appears coexisting with the "bustamite-like" phase to 1200°C.

INTRODUCTION

Inesite, a mineral not previously described from Australia, was, as far as the writers can ascertain, first observed on the 16 level of the Zinc Corporation mine at Broken Hill in 1949[2]. However, it was not until the latter half of 1962 when a vuggy vein, containing spectacular hemispherical masses of inesite, was intersected on the 19 level of the New Broken Hill Consolidated mine (N.B.H.C.), that the occurrence of this

[1] Present address: Department of Geochemistry and Mineralogy, Pennsylvania State University, University Park, Pennsylvania 16802.

[2] In October 1949 Mr. R. G. Whalan, then Inspector of Mines at Broken Hill, submitted to Mr. H. F. Whitworth of the Geological and Mining Museum, N.S.W. Department of Mines, a specimen tentatively identified by him as "mangano-pectolite". In about 1951 a portion of this sample (Mining Museum Cat. No. 22183) submitted to Dr. W. T. Schaller of the U. S. Geological Survey was correctly identified as inesite.

mineral became generally known. Subsequent discoveries of inesite have been made in the N.B.H.C. mine, the adjacent Zinc Corporation mine and the North Broken Hill mine (N.B.H.), about $1\frac{1}{2}$ miles north along the line-of-lode.

Occurrence

Inesite at Broken Hill occurs in post-ore, fracture-filled veins generally from 5–20 cm wide with rare local swellings up to 40 cm. Marginal to the veins the wall rock, consisting chiefly of calcium-manganese-iron silicates and lead-zinc sulphides, frequently shows considerable evidence of deformation. The deformed silicates are extensively altered to patches of fine-grained, greenish-brown chlorite. Locally, patches of this chlorite and recrystallized sulphides are enclosed in the veins.

Acicular crystals of inesite, generally less than 1–2 cm long, form radiating aggregates and together with white calcite predominate in the veins. In places veins consisting almost wholly of inesite become, within a few feet along strike, calcite-rich with minor inesite toward the centre.

In vuggy portions of the veins, such as on the 19 level of the N.B.H.C. mine, hemispherical masses of inesite up to 6 cm across, consisting of acicular, radiating crystals, are encrusted with striated, doubly-terminated crystals of colorless apophyllite. Rare, chisel-shaped, single crystals of inesite up to about $10\times3\times1$ mm have also been found lining the cavities at this locality, but irregular patches of sheaf-like aggregates of single crystals are more common. Crystals of apophyllite, generally less than 3 mm long, are studded on the surface of these aggregates.

At the N. B. H. mine a small quantity of very pale pink, granular apophyllite is associated with the inesite-calcite veins. Here, as elsewhere at Broken Hill, composite inclusions of galena-sphalerite-pyrite-chalcopyrite, up to 3 mm across, occur disseminated through the inesite-bearing veins.

Material Studied

Since 1963 the authors have made a collection of Broken Hill inesite and have had access to several private collections. Specimens from the following localities have been studied: (1) New Broken Hill Consolidated mine, 19 level (NBHC 1), (2) North Broken Hill mine, 24 level (NBH 1) and (3) North Broken Hill mine, 26 level (NBH 2).

Color and Hardness

Broken Hill inesite ranges from pale orange-pink to moderate pink-orange in color. On exposure to light and the atmosphere it darkens to a ginger-brown color. Single crystals from N.B.H.C. darken to an orange-red-brown.

The hardness of inesite is reported to be 6 in the literature following Schneider (1887). However, measurements on the (001), (010) and (100) pinacoids of Broken Hill crystals indicate a hardness of $5\frac{1}{2}$.

Morphological Crystallography

Inesite has been described previously from some nineteen localities where it typically forms aggregates of radiating acicular crystals. Terminated single crystals are rare having been recorded from only Langban, Sweden (Hamberg, 1894; Flink, 1900, 1916); Durango, Mexico (Farrington, 1900); Nanzenbach, Germany (Schneider, 1887) and Rendaiji, Japan (Takasu, 1955).

Table 1. Angle Table for Inesite from Broken Hill
Triclinic Pinacoidal

$a:b:c = 0.967:1:1.303$ $\quad \alpha = 92°14',\ \beta = 132°50',\ \gamma = 93°55'$
$p_0:q_0:r_0 = 1.349:0.096:1$ $\quad \lambda = 83°10',\ \mu = 46°44',\ \nu = 82°31'$
$p_0' = 1.857,\ q_0' = 1.318$ $\quad x_0' = 0.931,\ y_0' = 0.161$

Forms		ϕ	ρ	A	B	C
c	001	80°15′	43°22′	46°44′	83°10′	—
b	010	0°00′	90°00′	82°31′	—	83°10′
a	100	82°31′	90°00′	—	82°31′	46°44′
f	$2\bar{1}0$	244°28′	90°05′	161°57′	244°28′	50°07′
M	$1\bar{1}0$	120°42′	89°58′	38°11′	120°42′	59°30′
d	$0\bar{1}1$	141°50′	56°15′	64°54′	49°25′	47°34′
g	201	82°15′	77°44′	12°16′	82°26′	34°25′
h	$3\bar{1}1$	95°35′	81°34′	15°29′	84°28′	40°36′

Crystals from Nanzenbach, Langban and Durango are typically prismatic in habit whereas tabular and prismatic crystals from Rendaiji figured by Takasu have a "chisel-shape" strikingly similar to the rare single crystals from the 19 level of the N.B.H.C. mine (Fig. 1). The Broken Hill crystals range from 5–10 mm in length (along the morphological *c* axis) 1–3 mm in width (along the *b* axis) and about 1 mm thick. Only one, poorly preserved, doubly-terminated crystal has been observed at Broken Hill.

Ten single crystals were examined with a "Nedinsco" two-circle goniometer. The results are presented in Table 1, and the stereographic projection of the faces is shown in Fig. 3. The quality of reflections from the prominent faces is, in general, not perfect due to the presence of strong vertical striations on the *b* pinacoid and horizontal striations on the convexly curved *a* pinacoid. The *c* pinacoid and face *d* ($0\bar{1}1$) are crowded with numerous pits.

A very small, pitted face, omitted from Figure 1, occurs between *a* (100) and *d* ($0\bar{1}1$),

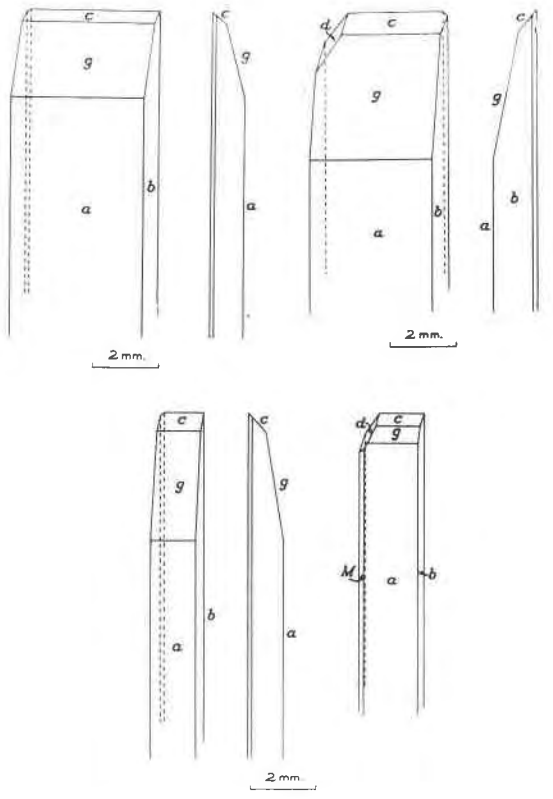

FIG. 1. Inesite crystals from Broken Hill.

but because of its size and poor preservation, accurate goniometric measurements could not be obtained. Measurements on the four crystals that have this face developed locate its pole to lie very close to the intersection of the zone [011] (containing *a* (100) and *d* ($0\bar{1}1$)) with the zone [$11\bar{2}$] (containing *g* (201) and *M* ($1\bar{1}0$)) (Fig. 3). Considering the quality of the reflected signal and the close proximity of the four measurements to the intersection of the above-mentioned zones, it is almost certain that the index of this face is ($3\bar{1}1$), a form not previously found on inesite. The Durango crystals described by Farrington also have a small face between *a* {100} and *d* {$0\bar{1}1$}, but this has been indexed as *s* {$9\bar{4}6$} and from Farrington's goniometric measurements is clearly distinct from *h* {$3\bar{1}1$}.

A list of the forms and the frequency of development of faces on crystals of inesite from Langban, Durango, Nanzenbach, Rendaiji and Broken Hill is given in Table 2. The previously reported forms *e* $\{\bar{1}01\}$, *l* $\{101\}$, *m* $\{110\}$, *j* $\{301\}$ and *n* $\{30\bar{1}\}$ are not developed on any of the Broken Hill crystals examined while $\bar{f}$ ($\bar{2}\bar{1}0$), not previously reported, is developed on 50 percent of Broken Hill crystals though *f* (210), a face common on Rendaiji crystals, is not developed.

TABLE 2. DEVELOPMENT AND FREQUENCY OF FORMS IN INESITE CRYSTALS

Form	Langban, Sweden			Durango Mexico	Nanzenbach Germany	Rendaiji Japan		Broken Hill Australia	
c 001	X[a,h]	X[b,h]	X[c,h]	X[d,h]	X[e,h]	X	10[f,g]	X	10[g]
b 010	X	X	X	X	X	X	10	X	10
a 100	X	X	X	X	X	X	10	X	10
f 210						X	1	X[i]	5
m 110			X						
M 1$\bar{1}$0					X	X	7	X	4
d 0$\bar{1}$1	X	X	X	X	X	X	2	X	6
g 201	X			X	X	X	2	X	7
j 301			X						
h 3$\bar{1}$1								X	4
e $\bar{1}$01		X	X	X	X	X	3		
l 101	X		X		X				
n 30$\bar{1}$	X								
o 532					X				
i $\bar{7}$47					X				
s 9$\bar{4}$6				X					

[a] Hamberg, 1894.
[b] Flink, 1900.
[c] Flink, 1916.
[d] Farrington, 1900.
[e] Schneider, 1887.
[f] Takasu, 1955.
[g] Frequency of development (:10).
[h] Frequency data not available.
[i] Face (210) absent but ($\bar{2}\bar{1}$0) present.
X—Form present.

None of the rare forms *o* $\{532\}$, *i* $\{\bar{7}47\}$, *s* $\{9\bar{4}6\}$ and *k* $\{\bar{1}\bar{1}.\ 0.\ 12\}$ occur on Broken Hill crystals. The latter form is most likely the more common *e* $\{\bar{1}01\}$.

The axial elements determined from the goniometric measurements given in Table 1 are in good agreement with the values obtained from X-ray single-crystal methods given in Table 4. However, due to the quality of the signal obtained from several of the crystal faces, the axial elements obtained by X-ray methods are considered to be more accurate.

CHEMICAL COMPOSITION

The three samples of inesite from Broken Hill were initially lightly crushed and hand-picked under the binocular microscope. The concentrate was recrushed under acetone and further concentrated using the Frantz isodynamic separator and then finally purified for analysis using heavy liquids.

TABLE 3. CHEMICAL ANALYSES OF BROKEN HILL INESITES

	1	2	3	4	5
SiO_2	45.48	45.47	45.58	44.52	9.96
MnO	33.24	33.27	34.38	36.80	6.16
FeO	3.03	3.33	2.46	0.65	.56
CaO	8.73	8.58	8.48	8.28	2.05
MgO	0.23	0.14	0.10	0.41	.08
Al_2O_3	0.19	0.22	0.25	0.28	.03
Na_2O	0.30	0.07	0.11	0.13	.06
K_2O	0.18	0.07	0.09	0.06	.03
H_2O^+	6.63	6.43	6.49	8.83	6.36
H_2O^-	2.10	2.19	2.22		
	100.11	99.77	100.16		

1. NBHC mine, Broken Hill (NBHC 1) (Analyst Ryall).
2. NBH mine, Broken Hill (NBH 1) (Ryall)
3. NBH mine, Broken Hill (NBH 2) (Ryall).
4. Average of thirteen analyses taken from the literature.
5. Number of "molecules" of oxide per unit cell (NBHC 1).

Silica was determined gravimetrically. Total iron and coprecipitated manganese were determined on separate aliquots obtained from the R_2O_3 precipitate. Alumina was determined by difference. The elements Mn, Ca, Fe, Mg, Na and K were determined using the atomic absorption method. Pb, Cu, Zn, Ba and Sr were also sought by this method but were not detected. Total water was determined by the Penfield method.

The chemical analyses of the three Broken Hill inesites are given in columns 1–3 of Table 3 where they are compared with the average of the thirteen most reliable analyses from the literature.

Broken Hill inesites are higher in iron and correspondingly lower in manganese when compared with previously analysed inesites. The most iron-rich inesite previously recorded was from Durango, Mexico with 2.48 percent FeO (Farrington, 1900). The high iron content of the Broken Hill inesites is in accord with high iron contents found in other calcium-manganese silicates from the Broken Hill lode (Smith, 1926; Henderson and Glass, 1936; Hutton, 1956; Stillwell, 1959).

UNIT CELL AND SPACE GROUP

The unit-cell parameters of the three inesites, derived from X-ray precession photographs (MoKα radiation) corrected for shrinkage, are given in Table 4 together with the unit-cell volumes and the calculated and observed specific gravities.

The unit cell chosen is the morphological one with the *c* axis parallel

TABLE 4. UNIT-CELL DATA FOR INESITES

	Morphological cell			Richmond cell Quinault (Richmond, 1942)
	NBHC 1	NBH 1	NBH 2	
α	91°48′ ± 05′[a]	91°58′ ± 05′[a]	91°56′ ± 05′[a]	87°38½′
β	132°35′	132°38′	132°38′	132°30′
γ	94°22′	94°09′	94°11′	97°05½′
a	8.927 ± .005 Å[a]	8.929 ± .005 Å[a]	8.927 ± .005 Å[a]	8.89 Å
b	9.245	9.239	9.242	9.14
c	11.954	11.948	11.946	12.14
$a:b:c$	0.9656:1:1.2930	0.9644:1:1.2931	0.9659:1:1.2926	0.973:1:1.328
Vol.	719.18 Å³	718.80 Å³	718.47 Å³	
G obs.	3.033	3.035	3.037	
G calc.	3.041	3.042	3.043	

[a] Average of 6 determinations.

to the elongation and the {010} and {100} cleavages. This cell has similar dimensions to that selected by Richmond (1942). The two cells, however, are not related by a simple 180° rotation about the c axis, as claimed by Richmond, since this can only be true if α and β are exactly 90°00′ and 135°00′, respectively. The α and β angles of inesite are not greatly different from these values, resulting in the morphological and Richmond cells having very similar, but not identical, dimensions.

The reduced cell for the N.B.H.C. material (given below) was transformed from the morphological cell by an algorithm method (Azaroff and Buerger, 1958) and is related to the morphological and Richmond cells (Fig. 2) by the transformation matrices:

Reduced→Richmond

$$\begin{vmatrix} 1 & 0 & 1 \\ 0 & \bar{1} & 0 \\ \bar{1} & 0 & 0 \end{vmatrix}$$

Reduced→Morphological

$$\begin{vmatrix} \bar{1} & 0 & 0 \\ 0 & 1 & 0 \\ 1 & 0 & 1 \end{vmatrix}$$

Reduced cell

$a = 8.927$ Å $\quad b = 9.245$ Å $\quad c = 8.842$ Å

$\alpha = 96°52'$ $\quad \beta = 84°32'$ $\quad \gamma = 94°22'$

Using Richmond's data, Donnay *et al.* (1963) derived a reduced cell related to the present cell by transposing the a and c cell edges and reversing the sense of α and β. Richmond's data, obtained from rotation and Weissenberg photographs about the axis of elongation of a tabular cleavage fragment, is not expected to result in unit-cell dimensions as

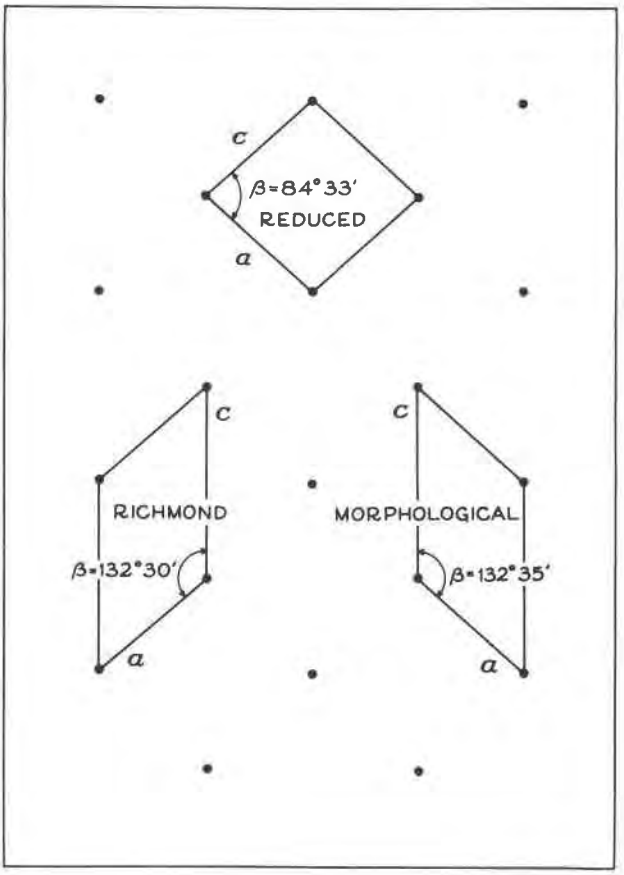

FIG. 2. Reduced, morphological and Richmond cells on the a–c plane.

accurate as those reported herein. The reduced cell derived from Richmond's data gives $a<c$, explaining the transformation of Donnay *et al.* whereas the cell derived from the present data gives $c<a$ requiring no transformation to conform to the accepted notation $c<a<b$.

Takasu (1955) concluded the space group of inesite to be $P1$ on the basis of positive piezoelectric tests using the apparatus described by Iitaka (1953). However, tests on inesite from Broken Hill and several other described localities carried out by the authors with a transmission-type piezoelectric detector (Blume, 1961) failed to detect piezoelectricity. Statistical tests using single-crystal X-ray intensity data ($N(z)$ and $P(y)$ tests) indicate inesite to be centrosymmetric and its space group is therefore $P\bar{1}$.

Chemical Formula

Richmond ascribed to inesite the generally accepted formula $Mn_7Ca_2Si_{10}O_{28}(OH)_2 \cdot 5H_2O$ and demonstrated its chemical and structural relationship to rhodonite. However, the high water content of Rendaiji inesite led Takasu (1955) to propose the formula $Mn_7Ca_2Si_{10}O_{28}(OH)_2 \cdot 6H_2O$. The difference in the formulas reflects the significant variation in the total water contents reported in inesite analyses—Richmond records 8.61 percent whereas Takasu records 9.48 percent. Total water contents reported in the literature range from 7.17 to 10.48 percent. Analyses with a water content of about 9.5 percent give rise to 36 oxygen and 14 hydrogen atoms per unit cell and the formula proposed by Takasu whereas those having a water content near the average (8.81%) give 35 oxygen and 12 hydrogen atoms per unit-cell and the Richmond formula.

Using the measured specific gravity of 3.033 (NBHC 1) there is one formula unit per unit cell. The molecular weight of the cell is 1317 a.m.u. and the cell content of the Broken Hill inesite given in Table 3 is in excellent agreement with that required by Richmond's formula.

The crystal structure analysis of inesite recently completed by one of us (W.R.R.) shows that the hydroxyl and water are coordinated to heavy cations so that the general formula is better written as $[Mn_7Ca_2(OH)_2(H_2O)_5]\ Si_{10}O_{28}$.

From the structural analysis it appears that the six water sites per unit cell may be partially occupied, thus explaining the wide range of water reported in chemical analyses of inesite.

The analysis of the N.B.H.C. inesite in Table 3 gives a formula

$$\left[\frac{(Mn_{6.16}Fe_{0.56}Mg_{0.08}Na_{0.12}Ca_{0.08})}{7.00}\ \frac{(Ca_{1.97}K_{0.06})}{2.03}\ (OH)_2(H_2O)_{5.36}\right] \frac{(Si_{9.96}Al_{0.06})}{10.02} O_{27.95}.$$

X-Ray Powder Data

The indexed X-ray powder data for inesite from Broken Hill is given in the first column of Table 7. The powder photograph was indexed using an Algol program for KDF9. Several indices give interplanar spacings close to measured values. The intensity of each of these was examined on single-crystal X-ray photographs and only those considered to be of sufficient intensity to be recorded on the powder photograph are included in the table. All lines have been indexed but, because of the high multiplicity, indices corresponding to spacings less than 2.00Å have been omitted.

Optical Properties

Larsen (1921) made the first detailed optical examination of inesite determining the refractive indices and the approximate optical orientation. Glass and Schaller (1939) examined inesite specimens from several localities but determined an orientation different to that of Larsen. Hutton (1941), working with New Zealand inesite, found its optical orientation agreed with that assigned by Larsen.

The difficulties experienced by the above-mentioned authors resulted in part from their having only radiating acicular specimens available for study. The Broken Hill material, however, provided terminated single crystals whose crystallographic directions were readily determined by X-ray methods permitting optical data obtained from them to be related unambiguously. The present results show that Larsen's and Hutton's results are correct. As suggested by Hutton, Glass and Schaller have transposed β and γ.

Inesite is biaxial negative with an optic angle near 76°. Fragments lying on the second best cleavage $\{100\}$ extinguish at approximately 14°30′ to the $\{010\}$ cleavage trace and give an optic axis at the edge of the field of view. Grains on the best cleavage $\{010\}$ extinguish at approximately 29°30′ to the $\{100\}$ cleavage and give a nearly centered Bx_a figure.

$\{010\}$ cleavage plates of the three Broken Hill inesites were measured using the universal stage and give $\alpha \wedge c = 74° \pm 1°$, $\beta \wedge c = 32° \pm 1°$, $\gamma \wedge c = 62° \pm 1°$. These measurements, shown in Figure 3, are similar to those of Hutton for New Zealand inesite. Universal stage determination of the optic angle on a number of $\{010\}$ cleavage plates were recorded orthoscopically and conoscopically using sodium light and the values corrected for mineral and segment refractive index differences. The results are given in Table 5.

Refractive indices determined for the three Broken Hill specimens by the double variation method on a five-axis universal stage (Emmons, 1943) are also listed in Table 5.

Thermal Decomposition in Air

In the first recorded examination of inesite at elevated temperatures. Richmond (1942) noted that the powder photograph of inesite heated to 800°C was "nearly identical" to that of rhodonite. In a subsequent brief study Yoshimura and Momoi (1960) ran the DTA curves of three Japanese inesites, reporting that inesite heated to 1200°C is converted to bustamite. Ito (1961) showed that on heating inesite passes through an amorphous state that gives rise to bustamite at about 800°C and cristobalite near 1100°C, both phases coexisting to 1200°C. Neither of the

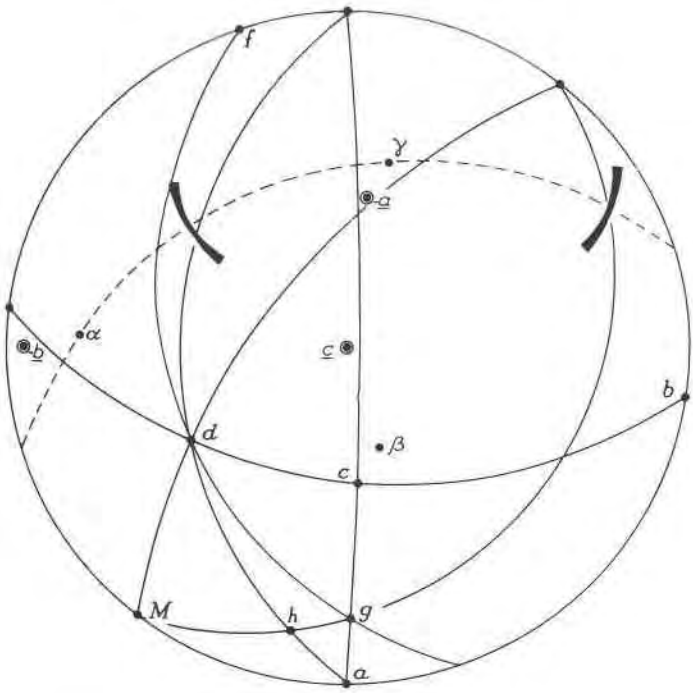

FIG. 3. Stereographic projection showing forms developed and optical orientation of Broken Hill inesite.

TABLE 5. OPTICAL PROPERTIES OF INESITES FROM BROKEN HILL

	NBHC 1	NBH 1	NBH 2
α	1.6178 ± .0003[a]	1.6179 ± .0003[a]	1.6183 ± .0003[a]
β	1.6384	1.6388	1.6390
γ	1.6519	1.6523	1.6526
γ-α	0.0341	0.0344	0.0343
α-β	0.0135	0.0135	0.0136
β-α	0.0206	0.0209	0.0207
$2V_x$ calc.	77°10′	76°52′	77°10′
$2V_x$ cono.	76°54′[b]	76°04′[b]	76°59′[b]
$2V_x$ ortho.	76°40′[b]	76°00′[b]	76°43′[b]
Dispersion	r>v weak	r>v weak	r>v weak
Pleochroism	nil	nil	nil

[a] At the sodium D line.
[b] Average of 4 measurements.

latter authors, however, detected the rhodonite phase described by Richmond.

A study of Broken Hill inesite using DTA, TGA, infrared absorption and X-ray powder methods shows that the thermal reactions are not as simple as previously reported.

The DTA curves 1 and 2, Figure 4, were obtained from the equipment described by Carthew and Cole (1953) using 0.18 gm of sample in a small metal block and 0.68 gm of sample in a large metal block, respec-

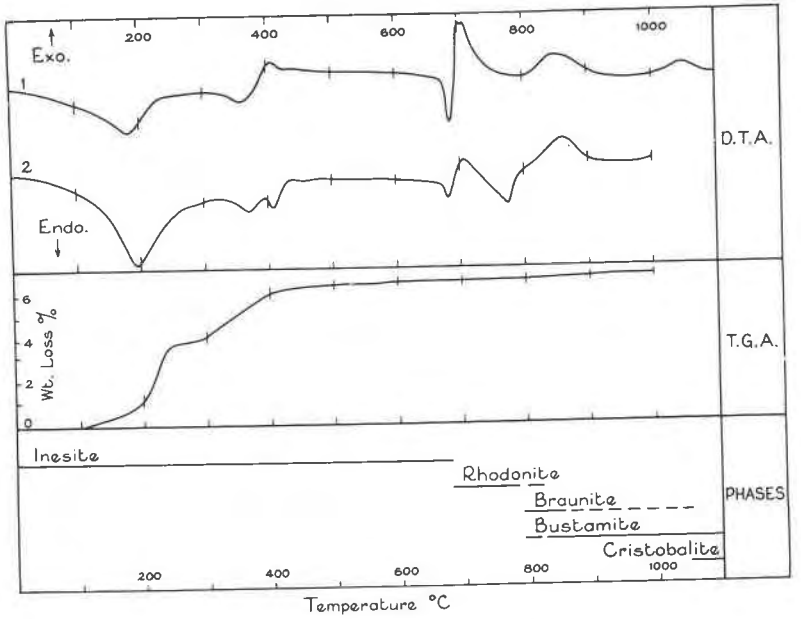

FIG. 4. DTA, TGA and phases present as inesite is heated in air.

tively. The two curves are similar and peak temperature correlation is good (Table 6) though better resolution is obtained using the larger sample, particularly between 350°–400°C and 600°–700°C.

A TGA using a 200-mg sample in the range 100°–1000°C was recorded with a Stanton thermobalance and is shown in Figure 4. Identical results were obtained from two runs.

X-ray powder data for phases at relevant temperatures are listed in Table 7, and the infrared spectra, obtained in the same manner as those reported by Ryall and Threadgold (1966), are shown in Figure 5 where they are compared with inesite (No. 1), rhodonite (No. 5) and bustamite (No. 9). Absorption peaks for inesite, rhodonite and bustamite have been assigned as follows:

TABLE 6. DTA PEAK TEMPERATURES OF INESITE FROM BROKEN HILL

Curve 1		Curve 2	
Endothermic	Exothermic	Endothermic	Exothermic
180 (s)		195 (s)	
372 (m)		355 (m)	
	406 (w)		396 (mw)
423 (w)		410 (m)	
686 (s)		683 (m)	
	705 (s)		709 (s)
790 (w)		775 (ms)	
	850 (ms)		862 (s)
	1050 (m)		
Recording terminated at 1200°		Recording terminated at 1000°C	

Relative intensity of peaks: s=strong; ms=medium strong, m=medium; mw=med. weak; w=weak.

3620–1640 cm^{-1}	(OH) stretching and bending
1087–937 cm^{-1}	(Si-O) stretching
773–549 cm^{-1}	(Si-O-Si) stretching
495–450 cm^{-1}	(M-O) stretching, (Si-O) bending

Changes produced on heating

0°–355°C. As inesite is heated to 355°C the DTA, TGA (Fig. 4) and the infrared curve (No. 2, Fig. 5) clearly show that water is gradually removed from the structure, but as evidenced by the infrared peak at 3620 cm^{-1} (No. 2, Fig. 5) the free OH is still retained up to 355°C.

Within this temperature range some oxidation occurs as evidenced by the color change to a pale red-brown.

355°–650°C. Over this temperature range continued oxidation results in a dark chocolate-brown color. Concomitant loss of residual OH occurring with the oxidation results in the TGA showing a net weight loss of about 0.3 percent.

Despite the weight loss of more than 6.5 percent up to 650°C the basic inesite chain structure still persists since the infrared curve, now devoid of peaks between 1600–3620 cm^{-1}, is recognizably inesite-like in character (*cf.* curves 1 and 2, Fig. 5). X-ray powder photographs are also remarkably similar to those of the natural material and to that heated to lower temperatures, though small shifts in spacings and changes in relative intensities of some lines are noted in Table 7.

By analogy with the dehydration of kaolinite, Ito (1961) used the

TABLE 7. X-RAY POWDER DATA FOR INESITE, HEATED INESITE, RHODONITE AND BUSTAMITE

Inesite						Rhodonite		Inesite			Bustamite	
Unheated				355° C		Unheated		1200° C			Unheated	
hkl[a]	*d*(calc) (Å)[b]	*d*(obs) (Å)[c]	*I*	*d*(obs) (Å)[c]	*I*	*d*(obs) (Å)[c]	*I*	*d*(obs) (Å)[c]	*I*	Ph[d]	*d* (obs) (Å)[c]	*I*
010	9.159	9.16	10	9.14	10							
$0\bar{1}1$	6.715	6.69	1			6.96	1	7.45	2	B	7.45	3
100	6.514	6.54	4	6.52	1						6.79	1
$11\bar{1}$	6.172	6.15	½									
$1\bar{1}2$	5.081	5.09	4	5.07	1							
020	4.580	4.59	5	4.58	2	4.73	3				4.78	1
$20\bar{2}$	4.434	4.44	½								4.42	3
002	4.373	4.38	½									
$02\bar{1}$	4.260	4.27	3									
$2\bar{1}\bar{2}$	4.098	4.10	1			4.12	3	4.05	3	C		
101	4.064											
$1\bar{2}0$	4.004	4.01	5	4.00	2							
$12\bar{1}$	3.964											
$1\bar{1}1$	3.916	3.89	1									
021	3.881											
$10\bar{3}$	3.794	3.79	1			3.82	2	3.73	5	B	3.71	5
012	3.783										3.60	1
$21\bar{1}$	3.593	3.62	1	3.62	1	3.53	3	3.42	6	B	3.42	6
111	3.542	3.55	1									
$1\bar{2}1$	3.266	3.26	1	3.26	1	3.32	4				3.33	1
200	3.258											
$2\bar{1}0$	3.206	3.20	1			3.23	1	3.21	7	B	3.22	7
$22\bar{2}$	3.086	3.10	1	3.10	1	3.12	5					
030	3.053	3.05	½			3.06	4					
$03\bar{1}$	2.989	2.96	½									
$20\bar{4}$	2.987											
$13\bar{1}$	2.947											
$1\bar{3}0$	2.197	2.92	8	2.91	8	2.94	10	3.01	7	B	3.01	6
003	2.915							2.90	10	B	2.88	10
$22\bar{1}$	2.896	2.88	1									
$2\bar{2}0$	2.838	2.84	8									
$13\bar{1}$	2.830											
$13\bar{2}$	2.756	2.73	7	2.72	7	2.75	7	2.71	4	B	2.70	2
304	2.730											
013	2.691	2.70	3									
314	2.634	2.63	2	2.63	2	2.67	3	2.63	1	B	2.64	2
112	2.620											
$1\bar{3}1$	2.617					2.59	3				2.56	2
$1\bar{2}2$	2.572	2.56	3	2.56	3	2.50	3					
$3\bar{2}\bar{2}$	2.555											

TABLE 7. (*Continued*)

Inesite						Rhodonite		Inesite		Bustamite	
Unheated				355° C		Unheated		1200° C		Unheated	
hkl[a]	*d*(calc) (Å)[b]	*d*(obs) (Å)[c]	*I*	*d*(obs) (Å)[c]	*I*	*d*(obs) (Å)[c]	*I*	*d*(obs) (Å)[c]	*I* Ph[d]	*d*(obs) (Å)[c]	*I*
$30\bar{1}$	2.554										
$3\bar{2}\bar{2}$	2.555	2.55	3								
$30\bar{1}$	2.554										
$3\bar{1}\bar{1}$	2.542										
$22\bar{4}$	2.540										
201	2.539										
$2\bar{1}1$	2.537										
$1\bar{2}4$	2.418	2.39	1	2.39	1	2.44	3	2.48	3 B	2.47	3
$2\bar{3}\bar{3}$	2.394							2.40	3 B	2.40	2
$31\bar{1}$	2.385										
$03\bar{2}$	2.380										
$32\bar{2}$	2.332	2.33	2	2.33	1	2.36	1	2.35	1 B	2.37	½
$23\bar{1}$	2.326							2.28	3 B	2.27	3
$3\bar{3}\bar{3}$	2.197	2.19	6	2.19	5	2.23	5	2.23	3 B	2.24	4
$41\bar{4}$	2.188										
$14\bar{1}$	2.183										
$1\bar{1}3$	2.172	2.17	4			2.18	3				
103	2.167										
$22\bar{5}$	2.136	2.13	1					2.13	3 B	2.12	3
$13\bar{4}$	2.114	2.12	1			2.11	1				
140	2.076	2.05	1	2.05	2	2.08	1				
123	2.063										
$42\bar{4}$	2.049										
$42\bar{3}$	2.045	2.04	1								
202	2.032										
		1.996	½							1.964	1
		1.971	1								
		1.938	1					1.925	1 B	1.926	2
		1.894	1	1.894	½	1.89	2			1.888	½
		1.848	1			1.87	2				
		1.838	2	1.839	3	1.83	1				
		1.772	1								
		1.764	½	1.762	½					1.814	½
		1.710	1			1.79	½	1.790	4 B	1.788	5
		1.692	1	1.692	4	1.73	2			1.755	1
		1.682	1			1.69	1	1.715	3 B	1.713	4
		1.650	3	1.651	2	1.67	2	1.665	4 B	1.667	4
		1.624	1			1.64	1				
		1.605	1	1.607	2	1.61	2			1.613	½
		1.600	1							1.555	3

TABLE 7. (*Continued*)

Inesite						Rhodonite		Inesite			Bustamite	
Unheated				355° C		Unheated		1200° C			Unheated	
hkl[a]	*d*(calc) (Å)[b]	*d*(obs) (Å)[c]	*I*	*d*(obs) (Å)[c]	*I*	*d*(obs) (Å)[c]	*I*	*d*(obs) (Å)[c]	*I*	Ph[d]	*d*(obs) (Å)[c]	*I*
		1.582	1			1.59	2	1.506	2	B	1.506	1
		1.566	1			1.56	½	1.475	½	B	1.475	1
		1.535	2	1.537	2	1.54	½	1.452	1	B	1.452	3
		1.493	2	1.495	1						1.444	1
		1.480	2	1.480	1	1.52	1				1.436	1
		1.443	1			1.48	4					
		1.428	2	1.427	3	1.45	1	1.420	1	B	1.423	1
		1.396	1	1.395	1	1.43	6				1.407	1
		1.373	2	1.373	2			1.363	1	B	1.363	1
		1.340	1					1.335	1	B	1.335	2
		1.323	1					1.296	1	B	1.297	1
		1.302	1								1.237	1
		1.278	1								1.229	1
		1.195	½								1.204	1
		1.177	½								1.198	1

[a] Refers only to unheated inesite and that heated to 355° and 650° C.
[b] Calculated from unit cell dimensions of NBHC inesite.
[c] Fe/Mn radiation, camera diam, 114.6 mm. corrected for film shrinkage.
[d] Phases present: R, rhondite; Br, braunite; B, bustamite; C, cristobalite.

term "metainesite" to describe the inesite phase formed before collapse of the structure. However, as inesite undergoes oxidation as well as dehydration yet still retains its fundamental structure to 650°C, a more appropriate analogy is to the similar thermal reactions of the fibrous iron-bearing amphiboles that result in the formation of the oxyamphiboles—*e.g.* "oxyamosite" (Addison *et al.* 1962; Hodgson *et al.* 1965a, b; Patterson, 1965). The term "oxyinesite" is therefore preferred to "metainesite" to describe the phase present on heating to near 650°C.

680°–1200°C. Disintegration of the oxyinesite, recrystallization of a new phase and a pronounced color change to brown-black take place between 685°–710°C. These processes are marked on the DTA curves by a prominent endotherm and the immediately following exotherm. However, the TGA in this region indicates no gain or loss of weight. An X-ray powder photograph at the peak temperature was rather nondescript but powder photographs and infrared spectra in the range 720°–760°C are very similar to those of rhodonite (Table 7 and Fig. 5).

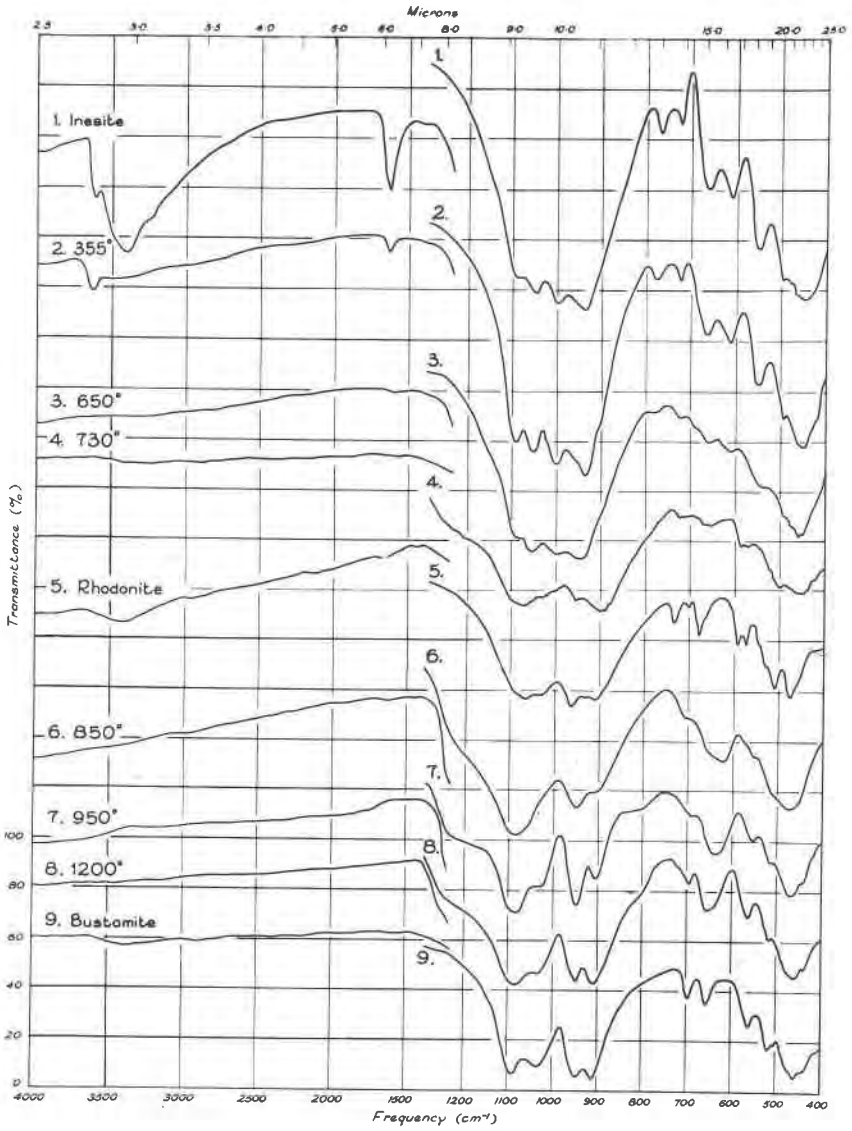

FIG. 5. Infrared absorption spectra of inesite, rhodonite, bustamite and heated inesite.

Though evidence of braunite is not detected by X-ray or infrared methods before 800°C, the marked color change observed in the range 685°–710°C may indicate the incipient development of braunite at about 100°C below the temperature at which it is obvious.

By 800°C the rhodonite-like phase has disappeared and is replaced by braunite and bustamite, the process being marked on the DTA by the endotherm near 780°C and the following exotherm near 850°–860°C. At 800°C braunite predominates over bustamite and lines on the X-ray powder photograph due to this phase are much stronger than those of bustamite. Examination of the 535–775 cm^{-1} region of the infrared spectrum at 850°C also confirms the predominance of braunite over bustamite since braunite peaks (705 (w), 622 (s, asymmetric), 550 cm^{-1} (sh,w)) mask the three characteristic bustamite peaks.

At 950°C the powder photograph and infrared spectrum closely resemble those of bustamite. Lines on the photograph are much sharper than at 800° and 850°C and peaks on the infrared spectrum are better resolved.

X-ray powder photographs indicate that as the temperature rises from 950°–1050°C the braunite phase diminishes until at about 1200°C it is almost absent. By this temperature the three peaks in the 535–775 cm^{-1} region of the infrared spectrum have shifted to very close to the frequencies for bustamite.

The presence of a new line at 4.05 Å, noted on powder photographs at 1050° and 1200°C, is interpreted as being due to the formation of cristobalite. Although the DTA shows an exotherm at 1050°C due to the crystallization of this phase, its presence is not detected on infrared spectra above 1050°C, since the bustamite-like phase is characterized by strong absorption in the 760–1300 cm^{-1} region where the prominent cristobalite peaks occur.

Discussion. Structurally inesite shows marked similarities to the rhodonite structure.[1] It is therefore not surprising that dehydrated inesite, which compositionally approximates a high-calcium rhodonite, inverts on heating to a rhodonite-like structure that in turn inverts to a bustamite-like structure. These observations agree with those of Liebau *et al.* (1958) who showed γ-$MnSiO_3$ (rhodonite structure) inverts at about 1160°C to β-$MnSiO_3$ (bustamite structure).

Dent Glasser and Glasser (1961) in their study of the thermal transformation of rhodonite conclude that near 1150°C rhodonite inverts to wollastonite. However, our investigations indicate that the transformation product of rhodonite is much more closely related to bustamite than to wollastonite. The powder photographs of bustamite and wollastonite are not greatly dissimilar but the photograph of this bustamite-

[1] The crystal structure of inesite and the mechanism of the transformation to rhodonite will be reported elsewhere.

TABLE 8. FREQUENCIES OF ABSORPTION MAXIMA OF HEATED INESITE PHASES COMPARED WITH RHODONITE AND BUSTAMITE (cm^{-1})

Band assignment	Inesite				Rhodonite	Inesite			Bustamite
	110°	355°	650°	730°	110°	850°	950°	1200°	110°
(M-O) stretching	450 s 462 sh, w	450 s 460 sh, w	454 s 463 s	450 s 488 m	458 s 495 s	470 s	442 sh, w 467 s	436 sh, w 450 s	435 sh, w 460 s
(Si-O) bending	475 sh, w 495 w	495 sh, w	495 sh, w	512 sh, w	514 sh, w 530 sh, w		516 sh, w	516 w	517 m
(Si-O-Si) stretching	549 m 611 m 663 m 727 m 773 m	549 m 612 m 662 m 725 m 775 m	545 m 612 m 662 m 725 m 785 m	555 w 575 w 663 m 695 w 720 w	559 m 579 m 667 m 694 m 720 m	550 sh, w 622 m 702 sh, w	555 m 635 m 690 w	560 m 656 m 693 m	562 m 656 m 695 m
(Si-O) stretching	937 vs 999 s 1050 s 1087 s	937 vs 999 s 1053 s 1090 s	940 vs 998 s 1050 s 1088 s	878 sh, w 895 s 946 s 1020 sh, w 1060 s	870 sh, w 895 s 950 vs 1025 s 1058 s 1075 sh, w	905 sh 950 s 1088 vs	905 s 950 vs 1035 w 1085 vs	908 vs 948 vs 1032 m 1085 vs	908 vs 945 vs 1035 s 1090 vs
(OH) bending & stretching	1640 s 3250 sh, w 3420 s 3620 s	1640 m 3420 w 3615 m							

Band intensity: vs—very strong; s—strong; m—medium; w—weak; sh—shoulder on a stronger band.

like phase near 1200°C resembles more closely bustamite than wollastonite. Further, the infrared spectrum (curve 8, Fig. 5) is remarkably similar to that of bustamite (curve 9 in Fig. 5 and Table 8) but significantly different than that of wollastonite (*cf.* curves 4 and 5, Fig. 1 in Ryall and Threadgold, 1966).

The possibility of an ordered bustamite structure existing at about 1200°C does, however, appear anomalous. If the cations in the bustamite-like phase at 1200°C are disordered, then the infrared spectra of the ordered and disordered bustamites are surprisingly similar.

ACKNOWLEDGMENTS

The authors are deeply indebted to Mr. Anthony Musgrave for his donation of the single crystals and the N.B.H.C. specimen used in the study. Other specimens used were collected by the authors on several trips to the Broken Hill mines and we wish to record our thanks to the management and staff of the mines for their assistance. In particular we would like to thank Messrs. B. Hawkins, Q. J. Henderson, A. Thomas and D. P. Watson for their personal interest and help.

Special thanks are due to Dr. W. F. Cole, C.S.I.R.O. Division of Building Research, who recorded a number of DTAs, Dr. R. A. Durie, C.S.I.R.O. Division of Coal Research, who provided ready access to infrared equipment and Dr. J. H. Patterson, Colonial Sugar Refining Co. Ltd., Research Laboratories, who ran DTAs and TGAs for the authors.

This work was carried out while one of us (W.R.R.) held a Commonwealth Post-Graduate Research Scholarship. Expenses incurred in the collection of material studied were defrayed by a research grant from the University of Sydney.

REFERENCES

AZAROFF, L. V., AND M. J. BUERGER (1958) *The Powder Method in X-ray Crystallography.* McGraw-Hill Book Co., New York, 136–141.

ADDISON, C. C., W. E. ADDISON, G. H. NEAL AND J. H. SHARP (1962) Amphiboles: I. The oxidation of crocidolite. *J. Chem. Soc.* (*London*), 1468–1471.

BLUME, B. J. (1961) Transmission-type piezoelectricity detector. *Rev. Sci. Instr.*, **32,** 598–599.

CARTHEW, A. R., AND W. F. COLE (1953) Differential thermal analysis equipment. *Aust. J. Instr. Tech.*, **9,** 23–30.

DONNAY, J. D. H., G. DONNAY, E. G. COX, O. KENNARD AND M. V. KING (1963) Crystal data. *Amer. Crystallogr. Ass. Monogr.*, **5,** 63.

EMMONS, R. C. (1943) The universal stage. *Geol. Soc. Amer. Mem.*, **8.**

FARRINGTON, O. C. (1900) New mineral occurrences. *Field Columbian Mus. Pub.* **44,** *Geol. Ser.* **1,** (7), 221–231.

FLINK, G. (1900) Mineralogische Notizen. *Bull. Geol. Inst. Univ. Upsala,* **5,** 81–96.

——— (1916) Ett par nyare af väl kristalliserade svenska mineral. *Geol. Fören. Stockholm Förh.*, **38,** 463–472.

GLASS, J. J., AND W. T. SCHALLER (1939) Inesite. *Amer. Mineral.*, **24,** 26–39.

GLASSER, L. S., DENT AND F. P. GLASSER (1961) Silicate transformations: rhodonite-wollastonite. *Acta Crystallogr.*, **14,** 818–822.

HAMBERG, A. (1894) Über den Inesit von Jacobsberg bei Nordmarken in Vermland. *Geol. Fören. Stockholm Förh.*, **16,** 323–327.

HENDERSON, E. P., AND J. J. GLASS (1936) Pyroxmangite, new locality: Identity of sobralite and pyroxmangite. *Amer. Mineral.*, **21,** 273–294.

HODGSON, A. A., A. G. FREEMAN AND H. F. W. TAYLOR (1965a) The thermal decomposition of crocidolite from Koegas, South Africa. *Mineral. Mag.*, **35,** 5–30.

——— (1965b) The thermal decomposition of amosite. *Mineral. Mag.*, **35,** 445–463.

HUTTON, C. O. (1941) Inesite from the Waihi mine, North Island, New Zealand. *Trans. Roy. Soc. N.Z.*, **71,** 99–101.

——— (1956) Manganpyrosmalite, bustamite and ferroan johannsenite from Broken Hill, N.S.W. *Amer. Mineral.*, **41,** 581–591.

IITAKA, Y. (1953) A technique for testing the piezoelectric properties of crystals. *Acta Crystallogr.*, **6,** 663–664.

ITO, K. (1961) Thermal transformation of inesite. *J. Jap. Ass. Mineral. Petrology Econ. Geol.*, **9,** 65–72.

LARSEN, E. S. (1921) The microscopic determination of the nonopaque minerals. *U.S. Geol. Surv. Bull.*, **679.**

LIEBAU, F., M. SPRUNG AND E. THILO (1958) Über das System $MnSiO_3$-$CaMn(SiO_3)_2$. *Z. Anorg. Allgem. Chem.*, **297,** 215–225.

PATTERSON, J. H. (1965) The thermal disintegration of crocidolite in air and vacuum. *Mineral. Mag.*, **35,** 31–37.

RICHMOND, W. E. (1942) Inesite, $Mn_7Ca_2Si_{10}O_{28}(OH)_2 \cdot 5H_2O$. *Amer. Mineral.*, **27,** 563–569.

RYALL, W. R., AND I. M. THREADGOLD (1966) Evidence for $[(SiO_3)_5]_\infty$ type chains in inesite as shown by X-ray and infrared absorption studies. *Amer. Mineral.*, **51,** 754–761.

SCHNEIDER, A. (1887) Das Vorkommen von Inesit und braunem Mangankeisel im Dillemburgischen. *Jahrb. Preuss. Geol. Landesanst.*, **9,** 472–496.

SMITH, G. (1926) A contribution to the mineralogy of New South Wales. *Dep. Mines (Geol. Surv.) N. S. W., Mineral Resour.*, **34,** 73.

STILLWELL, F. L. (1959) Petrology of the Broken Hill lode and its bearing on ore genesis. *Proc. Aust. Inst. Mining Met.*, **190,** 1–84.

TAKASU, S. (1955) On inesite from Rendaiji. *Mineral. J. (Tokyo)*, **1,** 242–249.

YOSHIMURA, T., AND H. MOMOI (1960) Inesite from the Kacho mine, Kochi Prefecture. *Kobutsugaku Zasshi*, **5,** 1–10.

Manuscript received, February 5, 1968; accepted for publication, June 19, 1968.